Available online at www.sciencedirect.com
ScienceDirect
Intermetallics 15 (2007) 1416–1424
Intermetallics
www.elsevier.com/locate/intermet

The Fe–Ni–Al phase diagram in the Al-rich (>50 at.% Al) corner

Igor Chumak*, Klaus W. Richter, Herbert Ipser

Department of Inorganic Chemistry/Materials Chemistry, University of Vienna, Währingerstraße 42, A-1090 Vienna, Austria

Received 20 February 2007; received in revised form 25 April 2007; accepted 29 April 2007
Available online 18 June 2007

Abstract

The ternary Fe–Ni–Al phase diagram between 50 and 100 at.% Al was investigated by a combination of powder X-ray diffraction (XRD), differential thermal analysis (DTA) and electron probe microanalysis (EPMA). Ternary phase equilibria and accurate phase compositions of the respective equilibrium phases were determined within the isothermal section at 850 °C. The crystal structure of τ1 ($Fe_{4-x}Ni_xAl_{10}$) and τ2 ($Fe_{2-x}Ni_xAl_9$) was determined by means of single crystal X-ray diffraction. The decagonal quasi-crystalline phase q ($Fe_{4.9}Ni_{23.4}Al_{71.7}$) was found to be stable between 850 °C and 930 °C. All experimental data were combined to yield a ternary reaction scheme (Scheil diagram) involving 10 ternary invariant reactions in the investigated composition range, and a liquidus surface projection was constructed based on DTA results.

Keywords: A. Aluminides, miscellaneous; B. Crystal chemistry of intermetallics; B. Phase diagrams

1. Introduction

The ternary Fe–Ni–Al system was investigated repeatedly due to interest in the specific properties of nickel aluminides (Ni-based shape memory alloys, super-alloys), and their possible modification with iron [1–4]. The most recent critical assessment of the Fe–Ni–Al phase diagram was carried out by Eleno et al. [5]. In spite of the broad interest and many experimental works, however, the information on phase equilibrium in the Fe–Ni–Al system is still not complete.

The Al-rich corner of the phase diagram was mainly investigated by Khaidar et al. [6], who determined the isothermal sections at 1050 °C, 950 °C and 750 °C (partially). The isothermal sections at 627 °C and 850 °C (partially) between 50 and 100 at.% Al were studied recently by Zhang et al. [7] (the isothermal section between 50 and 100 at.% Al at 850 °C investigated by us was already presented at the HTMC-XII [8]). The existence of the ternary compound Fe_3NiAl_{10} was determined at first by Bradley and Taylor [9] from X-ray powder diffraction. The authors stated that Fe_3NiAl_{10} is isotypic to Co_2Al_5 (Pearson symbol *hP*28, space group $P6_3/mmc$) but did not give the lattice parameters. The lattice parameters for this compound were later determined by Ellner and Röhrer [10] using a Guinier-method ($a = 7.703(1)$ Å, $c = 7.668(1)$ Å). As Khaidar et al. [6] were not able to index all reflections observed in their XRD experiments with the assumption of a Co_2Al_5-type structure, the true crystal structure of Fe_3NiAl_{10} is still unclear.

The crystal structure of the ternary compound $FeNiAl_9$ was not determined up to now. The lattice parameters for the $FeNiAl_9$ phase were calculated by Khaidar et al. [6], comparing the X-ray powder diffraction pattern of $FeNiAl_9$ with the pattern calculated for the Co_2Al_9-structure type (Pearson symbol *mP*22, space group $P2_1/c$).

An additional decagonal quasi-crystalline phase was detected in the Fe–Ni–Al system [11–15]. According to Ref. [12], this phase is stable in the temperature range 847–927 °C, the composition of this phase was given as $Fe_{5.4}Ni_{23.0}Al_{71.6}$. Recently, however, de Laissardiere et al. [16] based on ab initio band structure calculations, stated in a review paper that the decagonal quasi-crystalline phase in the Fe–Ni–Al system is to be regarded as metastable.

* Corresponding author.
E-mail address: chumak_i@yahoo.de (I. Chumak).

0966-9795/$ - see front matter © 2007 Elsevier Ltd. All rights reserved.
doi:10.1016/j.intermet.2007.04.012

Table 1
The nominal compositions, phase compositions and lattice parameters of identified phases at 850 °C

Nominal composition (at.%)			Phase identified	Lattice parameters (Å)			Phase composition determined by EPMA (at.%)		
Fe	Ni	Al		*a*	*b*	*c*	Fe	Ni	Al
35	5	60	B2	2.9041(1)			37.9(1)	9.1(1)	53.0(2)
			$FeAl_2$	4.8757(4)	6.4612(8)	8.7990(6)	32.2(1)	1.3(1)	66.5(1)
				$\alpha = 91.79(1)$	$\beta = 73.28(1)$	$\gamma = 96.81(1)$			
32.5	7.5	60	B2	2.8884(1)			32.8(1)	14.2(1)	53.0(1)
			$FeAl_2$	4.8780(3)	6.4612(5)	8.8004(6)	31.4(1)	2.3(1)	66.3(1)
				$\alpha = 91.749(7)$	$\beta = 73.271(7)$	$\gamma = 96.890(8)$			
			Fe_2Al_5	7.6613(7)	6.4225(3)	4.2156(3)	29.0(1)	1.2(1)	69.8(2)
30	10	60	B2	2.8863(1)			30.9(2)	15.2(2)	53.9(1)
			Fe_2Al_5	7.6415(3)	6.4147(2)	4.2187(2)	28.3(1)	0.8(1)	70.9(1)
25	15	60	B2	2.8840(1)			26.2(1)	19.4(1)	54.4(1)
			τ1	7.6995(3)		7.6900(8)	22.9(1)	6.4(1)	70.7(1)
20	20	60	B2	2.8714(1)			–	–	–
			τ1	7.6896(1)		7.6896(1)	–	–	–
15	25	60	B2	2.8638(1)			13.2(1)	30.8(1)	56.0(1)
			τ1	7.6918(2)		7.6864(3)	20.5(1)	8.3(1)	71.2(1)
10	30	60	B2	2.8627(1)			–	–	–
			τ1	7.7006(3)		7.6776(3)	–	–	–
			Ni_2Al_3	4.0458(2)		4.9062(4)	–	–	–
7.5	32.5	60	B2	2.8609(1)			8.0(1)	36.3(2)	55.7(1)
			τ1	7.705(1)		7.680(2)	18.8(4)	10.9(1)	70.3(4)
			Ni_2Al_3	4.0434(1)		4.9086(1)	4.2(1)	38.1(2)	57.7(2)
5	35	60	Ni_2Al_3	4.0473(1)		4.9148(1)	3.9(1)	36.0(2)	60.1(1)
			τ1	7.7132(5)		7.6608(7)	18.5(3)	9.4(3)	72.1(1)
29	4	67	B2	2.8870(1)			30.6(1)	15.0(2)	54.4(2)
			Fe_2Al_5	7.6509(3)	6.4242(2)	4.2229(2)	28.0(1)	1.1(1)	70.9(1)
26	7	67	B2	2.8832(1)			28.9(1)	16.9(1)	54.2(1)
			τ1	7.6717(4)		7.7195(3)	23.6(1)	5.9(2)	70.5(2)
			Fe_2Al_5	7.6716(8)	6.4264(3)	4.2139(4)	27.9(1)	1.2(1)	70.9(1)
24	9	67	B2	2.8848(1)			27.0(1)	18.3(2)	54.7(2)
			τ1	7.6868(2)		7.7239(2)	23.1(1)	6.0(1)	70.9(1)
20	13	67	B2	2.8676(1)			16.3(1)	28.1(1)	55.6(1)
			τ1	7.6922(2)		7.6873(2)	21.2(1)	7.6(1)	71.2(1)
15	18	67	B2	2.8580(1)			–	–	–
			τ1	7.7000(1)		7.6738(1)	–	–	–
			Ni_2Al_3	4.0418(1)		4.9053(1)	–	–	–
12.5	20.5	67	τ1	7.7061(1)		7.6783(2)	18.7(2)	9.6(1)	71.7(2)
			Ni_2Al_3	4.0439(1)		4.9078(2)	3.7(2)	37.0(4)	59.3(3)
10	23	67	τ1	7.7024(1)		7.6725(1)	18.8(1)	9.6(1)	71.6(1)
			Ni_2Al_3	4.0411(1)		4.9043(2)	3.5(1)	37.0(1)	59.5(1)
5	28	67	Ni_2Al_3	4.016(1)		4.871(1)	1.2(1)	37.7(2)	61.1(2)
			Fe_4Al_{13}	15.4482(8)	8.0394(3)	12.4847(5)	17.7(1)	7.0(2)	75.3(2)
					$\beta = 107.724(2)$				
25.5	3	71.5	τ1	7.6781(1)		7.7131(1)	23.1(2)	5.6(1)	71.3(3)
			Fe_2Al_5	7.6718(5)	6.4245(4)	4.2131(3)	27.2(2)	0.9(1)	71.9(3)
21.5	7	71.5	τ1	7.6859(1)		7.6904(1)	21.8(2)	6.3(1)	71.9(1)
18.5	10	71.5	τ1	7.6804(1)		7.6947(1)	18.5(3)	9.9(2)	71.6(3)
			Ni_2Al_3				4.7(1)	36.3(1)	59.0(1)
15	13.5	71.5	τ1	7.6762(1)		7.7144(1)	15.7(3)	11.5(4)	72.0(4)
			Ni_2Al_3				2.3(2)	36.6(2)	61.0(3)

(*continued on next page*)

Table 1 (*continued*)

Nominal composition (at.%)			Phase identified	Lattice parameters (Å)			Phase composition determined by EPMA (at.%)		
Fe	Ni	Al		*a*	*b*	*c*	Fe	Ni	Al
12.5	16	71.5	τ1	7.7049(1)		7.6422(1)	15.8(2)	12.9(1)	71.3(2)
			Ni_2Al_3	4.0473(1)		4.9012(1)	1.8(1)	38.2(1)	60.0(1)
			Fe_4Al_{13}	15.436(2)	8.090(1) $\beta = 107.68(1)$	12.424(2)	17.0(3)	8.2(4)	74.8(1)
10	18.5	71.5	Fe_4Al_{13}	15.530(2)	8.040(1) $\beta = 107.43(1)$	12.534(2)	16.1(1)	8.9(1)	75.0(1)
			Ni_2Al_3	4.0482(1)		4.8999(2)	1.8(2)	37.0(2)	61.2(2)
7	21.5	71.5	Fe_4Al_{13}	15.484(3)	8.069(1) $\beta = 107.76(1)$	12.474(2)	13.8(1)	10.7(1)	75.5(2)
			Ni_2Al_3	4.0550(1)		4.9025(2)	0.6(1)	37.0(2)	62.4(2)
			q				4.9(1)	23.4(1)	71.7(1)
5	23.5	71.5	q				4.9(1)	23.4(1)	71.7(1)
2.5	26	71.5	Ni_2Al_3	4.0542(1)		4.9029(1)	–	–	–
			$NiAl_3$	6.550(3)	7.354(2)	4.873(1)	–	–	–
			q				–	–	–
20	5	75	Fe_4Al_{13}	15.508(2)	8.078(1) $\beta = 107.50(2)$	12.478(3)	20.2(1)	4.4(3)	75.4(1)
			τ1	7.636(4)		7.705(4)	18.4(1)	9.5(1)	72.1(1)
15	10	75	Fe_4Al_{13}	15.463(6)	8.1040(4) $\beta = 107.105(3)$	12.4558(7)	15.6(1)	9.0(1)	75.4(2)
			Ni_2Al_3	4.0535(2)		4.9794(4)	2.0(2)	36.3(2)	61.6(3)
10	15	75	Fe_4Al_{13}	15.466(1)	8.051(2) $\beta = 107.88(1)$	12.478(1)	–	–	–
			$NiAl_3$	6.646(1)	7.357(1)	4.805(1)	–	–	–
			q				–	–	–
5	20	75	Fe_4Al_{13}	15.465(1)	8.053(1) $\beta = 107.87(1)$	12.477(1)	13.7(1)	10.9(1)	75.4(1)
			$NiAl_3$	6.6458(4)	7.3586(6)	4.8040(2)	2.0(1)	22.6(1)	75.4(1)
			q				4.9(1)	23.4(1)	71.7(1)
15	5	80	Fe_4Al_{13}	15.496(1)	8.102(1) $\beta = 107.32(1)$	12.443(1)	18.8(3)	4.8(3)	76.4(2)
			L[c]				–	–	–
10	10	80	Fe_4Al_{13}	15.3637(8)	8.1403(6) $\beta = 107.784(2)$	12.4329(8)	–	–	–
			L[c]				–	–	–
5	15	80	Fe_4Al_{13}	15.464(3)	8.080(2) $\beta = 107.78(2)$	12.464(3)	14.3(1)	10.1(2)	75.6(2)
			$NiAl_3$	6.6425(3)	7.3615(3)	4.8053(2)	2.1(1)	22.7(1)	75.2(1)
			L[c]				–	–	–
4.9[a]	23.4	71.7	Fe_4Al_{13}	15.477(4)	8.082(2) $\beta = 107.71(2)$	12.468(3)	–	–	–
			$NiAl_3$	6.6354(2)	7.3647(2)	4.8114(1)	–	–	–
			Ni_2Al_3	4.0513(1)		4.9003(2)	–	–	–
8[a]	14	78	Fe_4Al_{13}	15.481(4)	8.083(3) $\beta = 107.66(4)$	12.476(9)	–	–	–
			$NiAl_3$	6.6260(4)	7.3633(6)	4.8082(3)	–	–	–
			τ2	6.2388(3)	6.3004(4) $\beta = 95.093(5)$	8.5983(5)	–	–	–
6.3[b]	11.7	82	τ2	6.2406(1)	6.2993(1) $\beta = 95.129(1)$	8.5992(1)	–	–	–

Note that only selected samples were investigated by EPMA.

[a] Annealed at 700 °C.

[b] Annealed at 750 °C.

[c] The composition of the liquid could not be determined by EPMA.

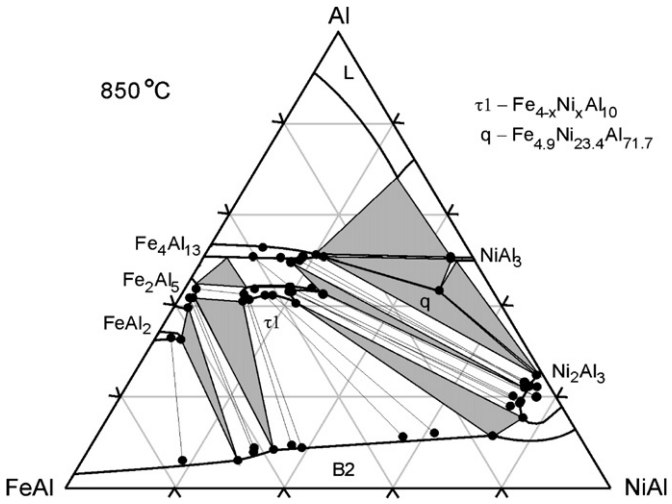

Fig. 1. Isothermal section of the Fe–Ni–Al system between 50 and 100 at.% Al at 850 °C with experimental tie-lines and triangles (black circles: phase compositions measured by EPMA).

The knowledge of the invariant reactions in the Fe–Ni–Al system is not complete. Three ternary invariant reactions in the Al-rich corner are described by Schrader and Hanemann [17], i.e., P: $[L + (Fe_4Al_{13}) + (NiAl_3)] = \tau 2$ at 809 °C (composition of liquid (L) – 2.11, 10.83, 87.06 at.% Fe, Ni and Al, respectively); U: $[L + (Fe_4Al_{13})] = [\tau 2 + (Al)]$ at 650 °C (composition of L – 0.795, 0.786, 98.42 at.% Fe, Ni and Al, respectively); E: $L = [(NiAl_3) + \tau 2 + (Al)]$ at 638 °C (composition of L – 0.105, 3.175, 96.72 at.% Fe, Ni and Al, respectively). The reactions involving the Fe_3NiAl_{10} and decagonal quasi-crystalline phase between 847 °C and 1340 °C are unknown.

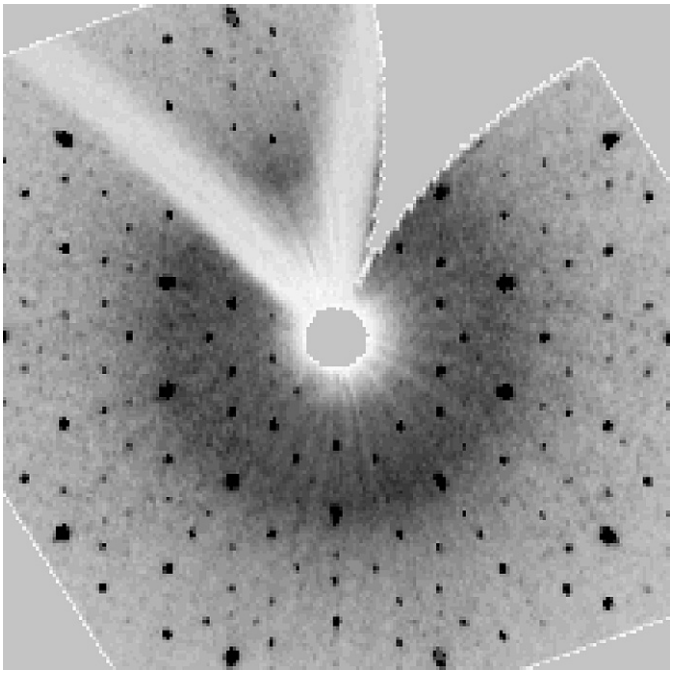

Fig. 2. Laue diffraction pattern of the quasi-crystal $Fe_{4.9}Ni_{23.4}Al_{71.7}$ showing the decagonal symmetry.

Table 2
Crystal data and structure refinement for $Fe_{4-x}Ni_xAl_{10}$ (τ1) and $Fe_{2-x}Ni_xAl_9$ (τ2)

Empirical formula	$Fe_{2.67}Ni_{1.43}Al_{9.90}$	$Fe_{0.7}Ni_{1.3}Al_9$
Temperature (K)	293	
Radiation and wavelength	Mo, 0.71069 Å	
Diffractometer	CAD4	
Structure type	Co_2Al_5	Co_2Al_9
Crystal system (space group)	Hexagonal, $P6_3/mmc$	Monoclinic, $P2_1/c$
Unit cell parameters[a] (Å)	$a = 7.70937(5)$ $c = 7.67947(8)$	$a = 6.2406(1)$ $b = 6.2993(1)$ $c = 8.5992(1)$ $\beta = 95.129(1)$
Volume (Å^3)	394.4(1)	336.70(1)
Z, Calculated density (g/cm^3)	2, 4.188	2, 3.549
Absorption coefficient, mm^{-1}	8.707	6.550
$F(000)$	473	172
2θ Range for data collection	8.10–58.06	6.56–65.48
Reflections collected/unique	7072/231	3259/1141
Refinement method	Full-matrix least-squares on F^2	Full-matrix least-squares on F^2
Data/parameters	231/23	1141/54
Goodness-of-fit on F^2	1.284	0.699
Final R indices $[I > 2\sigma(I)]$	$R1 = 0.0326$, $wR2 = 0.0653$	$R1 = 0.0334$, $wR2 = 0.0523$
R Indices (all data)	$R1 = 0.0358$, $wR2 = 0.0663$	$R1 = 0.0878$, $wR2 = 0.0558$
Extinction coefficient	0.004(2)	0.013(1)
Largest diff. peak and hole, eA^{-3}	0.933 and −0.833	0.843 and −0.652

[a] Lattice parameters calculated from Guinier powder data.

2. Experimental

Samples with a total mass of 500 mg were prepared from aluminum rod (99.999%, Alfa, Karlsruhe, Germany), iron foil (99.99%, Advent Res., Halesworth, UK) and nickel foil (99.99%, Advent Res., Halesworth, UK). Calculated amounts of the elements were weighed to an accuracy of 0.05 mg and arc melted on a water-cooled copper plate under an argon atmosphere. Zirconium was used as a getter material within the arc chamber. The samples were re-melted one or two times and then weighed back in order to check for possible mass losses (which were generally found to be negligible). For equilibration the alloys were then annealed for 2–3 weeks at 850 °C in alumina crucibles that were sealed into evacuated quartz glass ampoules. Annealing time for the alloys at 750 °C and 700 °C was 3 weeks. After quenching in water, the samples were investigated by means of X-ray diffraction (XRD), differential thermal analysis (DTA) and electron microprobe analysis (EPMA).

Initial sample characterization was performed by X-ray powder diffraction, using the Guinier technique (Cu $K\alpha_1$ radiation). The unit cell parameters were refined using the program TOPAS V3 [18]. High purity silicon was used as internal standard for the lattice parameter determination.

DTA measurements were carried out on a DTA 404S/3 (Netzsch, Selb, Germany) using open alumina crucibles and

Table 3
Atomic coordinates and displacement parameters (Å$^2 \times 10^3$) for $Fe_{4-x}Ni_xAl_{10}$ (τ1) and $Fe_{2-x}Ni_xAl_9$ (τ2)

Atom	Site	*x*/*a*	*y*/*b*	*z*/*c*	U_{eq}	U_{11}	U_{22}	U_{33}	U_{23}	U_{13}	U_{12}
$Fe_{4-x}Ni_xAl_{10}$ (τ1)											
M1	2*a*	0	0	0	7(1)	8(1)	8(1)	6(2)	0	0	4(1)
Al2	6*h*	0.4638(1)	2*x*	1/4	9(1)	8(1)	11(1)	10(1)	0	0	5(1)
Al3	12*k*	0.1943(1)	0.3885(2)	0.9401(2)	9(1)	9(1)	9(1)	8(1)	1(1)	1(1)	5(1)
M2	2*d*	1/3	2/3	3/4	7(1)	7(1)	7(1)	6(1)	0	0	4(1)
M3	6*h*	0.1252(1)	2*x*	1/4	7(1)	9(1)	5(1)	5(1)	0	0	3(1)
M1 = 0.903(1) Al + 0.097(1) Fe/Ni (from refinement); M2 = M3 = 0.65 Fe + 0.35 Ni (from EPMA)											
$Fe_{2-x}Ni_xAl_9$ (τ2)											
Al1	4*e*	0.0886(2)	0.7106(2)	0.2301(2)	13(1)	13(1)	13(1)	13(1)	4(1)	0(1)	1(1)
Al2	4*e*	0.2122(2)	0.3875(2)	0.0429(1)	12(1)	12(1)	13(1)	10(1)	−3(1)	1(1)	−1(1)
Al3	4*e*	0.4041(2)	0.0287(2)	0.2679(2)	14(1)	14(1)	13(1)	14(1)	1(1)	4(1)	−1(1)
Al4	4*e*	0.6098(2)	0.1950(2)	0.0040(2)	12(1)	12(1)	12(1)	13(1)	−1(1)	−1(1)	0(1)
M	4*e*	0.26434(1)	0.3798(1)	0.3333(1)	11(1)	11(1)	11(1)	12(1)	0	1(1)	0(1)
Al5	2*a*	0	0	0	15(1)	17(1)	11(1)	19(1)	−2(1)	9(1)	−2(1)
M = 0.35 Fe + 0.65 Ni from nominal sample composition											

U_{eq} is defined as one-third of the trace of the orthogonalized U_{ij} tensor. The anisotropic displacement factor exponent takes the form: $-2\pi^2[h^2a^{*2}U_{11} + \cdots + 2hka^*b^*U_{12}]$.

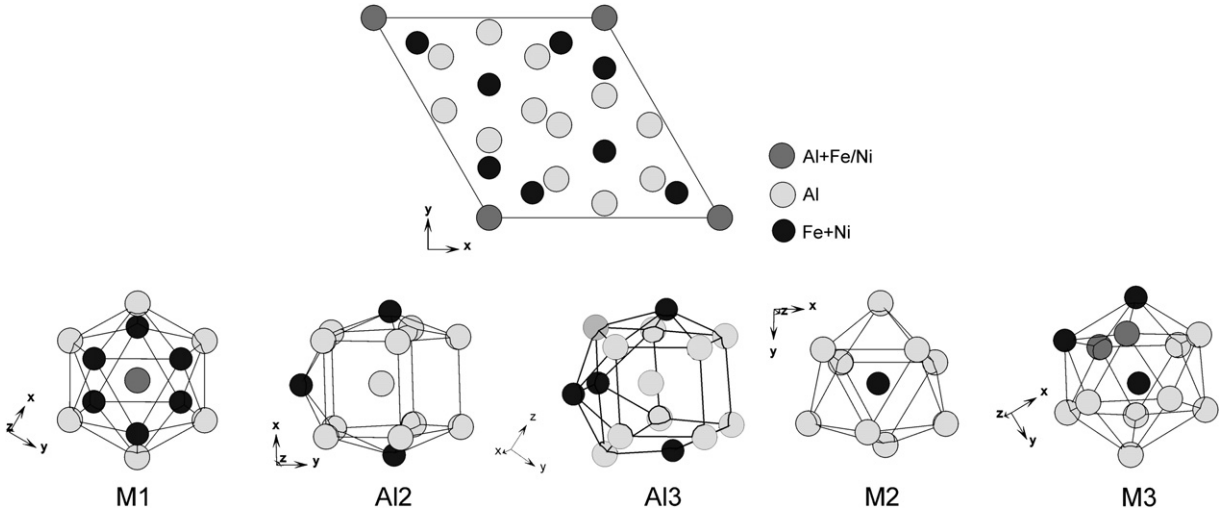

Fig. 3. Unit cell and coordination polyhedra of the atoms in the $Fe_{4-x}Ni_xAl_{10}$ structure.

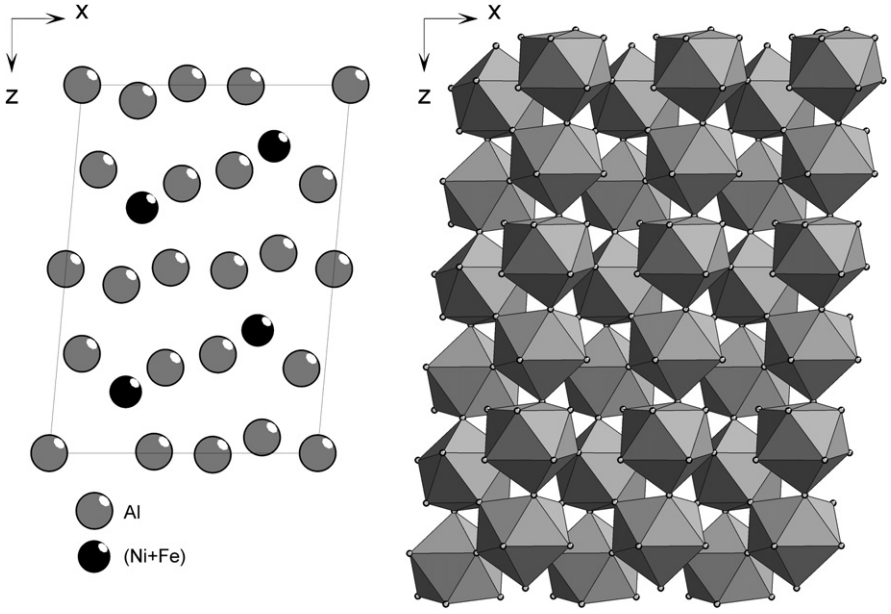

Fig. 4. Unit cell and arrangement of the [MAl_9]-polyhedra in the $Fe_{2-x}Ni_xAl_9$ structure.

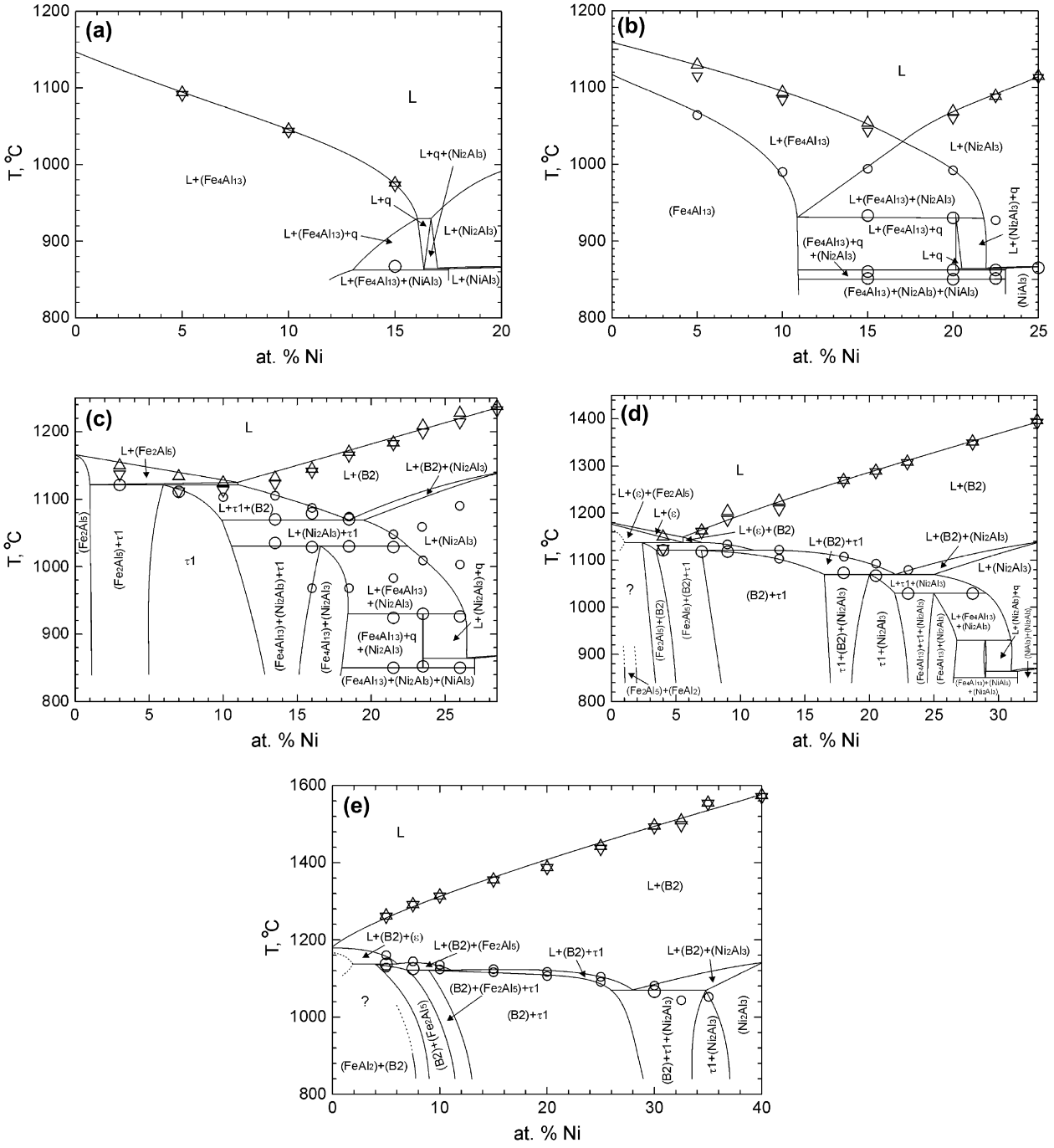

Fig. 5. Vertical sections in Fe–Ni–Al at: (a) 80 at.% Al, (b) 75 at.% Al, (c) 71.5 at.% Al, (d) 67 at.% Al and (e) 60 at.% Al. Large circles: invariant thermal effects; triangles up: liquidus on heating; triangles down: liquidus on cooling; small circles: other thermal effects.

employing a slow permanent argon flow. A sample mass of approximately 200 mg was used for the experiments and the samples were checked routinely for possible mass changes during the DTA experiment. Two heating- and cooling-curves were recorded for each sample using a heating rate of 5 K min^{-1}. The Pt/Pt10%Rh thermocouples of the DTA instrument were calibrated at the melting points of high purity Ni, Au and In.

The composition of the individual phases at 850 °C was determined by EPMA on a Cameca SX electron probe 100 (Cameca, Courbevoie, France) using wavelength dispersive spectroscopy (WDS) for quantitative analyses and employing pure aluminum, iron and nickel as standard materials. The measurements were carried out at 15 kV using a beam current of 20 nA. Conventional ZAF matrix correction was used to calculate the final composition from the measured X-ray intensities.

3. Results and discussion

3.1. Isothermal section at 850 °C

The isothermal section of the Fe–Ni–Al phase diagram between 50 and 100 at.% Al at 850 °C was studied on 33

Table 4
Ternary phase reactions observed by DTA

Reaction	T (°C)	Phase	Composition (at.%)		
			Fe	Ni	Al
P_1: L + (Fe_4Al_{13}) + ($NiAl_3$) = τ2	809	L	2	11	87
		Fe_4Al_{13}	14	11	75
		$NiAl_3$	2	23	75
		τ2	6.5	11.5	82
E_2: q = (Fe_4Al_{13}) + ($NiAl_3$) + (Ni_2Al_3)	850	q	4.9	23.4	71.7
		Fe_4Al_{13}	14	11	75
		$NiAl_3$	2	23	75
		Ni_2Al_3	2	37	61
U_2: L + q = (Fe_4Al_{13}) + ($NiAl_3$)	860	L	3	14	83
		q	4.9	23.4	71.7
		Fe_4Al_{13}	14	11	75
		$NiAl_3$	2	23	75
U_3: L + (Ni_2Al_3) = q + ($NiAl_3$)	864	L	3	15	82
		Ni_2Al_3	2	37	61
		q	4.9	23.4	71.7
		$NiAl_3$	2	23	75
P_2: L + (Fe_4Al_{13}) + (Ni_2Al_3) = q	930	L	4	17	79
		Fe_4Al_{13}	14	11	75
		Ni_2Al_3	1.5	37	61.5
		q	4.9	23.4	71.7
U_4: L + τ1 = (Fe_4Al_{13}) + (Ni_2Al_3)	1030	L	8	17	75
		τ1	18	10.5	71.5
		Fe_4Al_{13}	17	8	75
		Ni_2Al_3	1	37	62
U_5: L + (B2) = (Ni_2Al_3) + τ1	1069	L	10	17	73
		B2	12.5	30	57.5
		Ni_2Al_3	5	35	60
		τ1	28.5	10	71.5
U_6: L + (Fe_2Al_5) = (Fe_4Al_{13}) + τ1	~1116	L	17.5	8	74.5
		Fe_2Al_5	27	1	72
		Fe_4Al_{13}	24	1	75
		τ1	22.5	6	71.5
P_3: L + (Fe_2Al_5) + (B2) = τ1	1121	L	17	11	72
		Fe_2Al_5	26.5	1	72.5
		B2	36	11	53
		τ1	22.5	6	71.5
U_7: L + (ε) = (Fe_2Al_5) + (B2)	1137	L	22	8	70
		ε	37.5	1	61.5
		Fe_2Al_5	27.5	1	71.5
		B2	40	5	55

samples in sections at 60, 67, 71.5, 75 and 80 at.% Al, respectively. The results of XRD and EPMA analysis are summarized in the Table 1 and a graphical representation of phase equilibria is given in Fig. 1. Two ternary compounds were found at this temperature: τ1 ($Fe_{4-x}Ni_xAl_{10}$) and the decagonal quasi-crystalline phase q. While $Fe_{4-x}Ni_xAl_{10}$ shows an extended range of homogeneity corresponding to $0.78 \leq x \leq 1.80$ (lattice parameter variation: $a = 7.6781(1)$–$7.7049(1)$ Å, $c = 7.7131(1)$–$7.6432(1)$ Å), the quasi-crystalline phase q was found at only one specific composition $Fe_{4.9}Ni_{23.4}Al_{71.7}$ which is in excellent agreement with the composition given in Ref. [13]. Fig. 2 shows the Laue diffraction pattern of q (crystal extracted from sample $Fe_5Ni_{23.5}Al_{71.5}$) along the decagonal axis, clearly revealing the quasi-crystalline character of this compound. As the phase q was found in well-annealed samples, the thermodynamic stability of this phase with respect to decomposition into its neighboring phases is clearly confirmed. The solubility of the corresponding third component in the binary compounds Fe_2Al_5, $FeAl_2$ and $NiAl_3$ was found to be small (1 and 2 at.% Ni and 2 at.% Fe, respectively). The solid solutions based on the binary Ni_2Al_3 and Fe_4Al_{13} are larger. The homogeneity range of Ni_2Al_3 in the ternary system is up to 4 at.% Fe, the maximal solubility of Ni in Fe_4Al_{13} is 11 at.%.

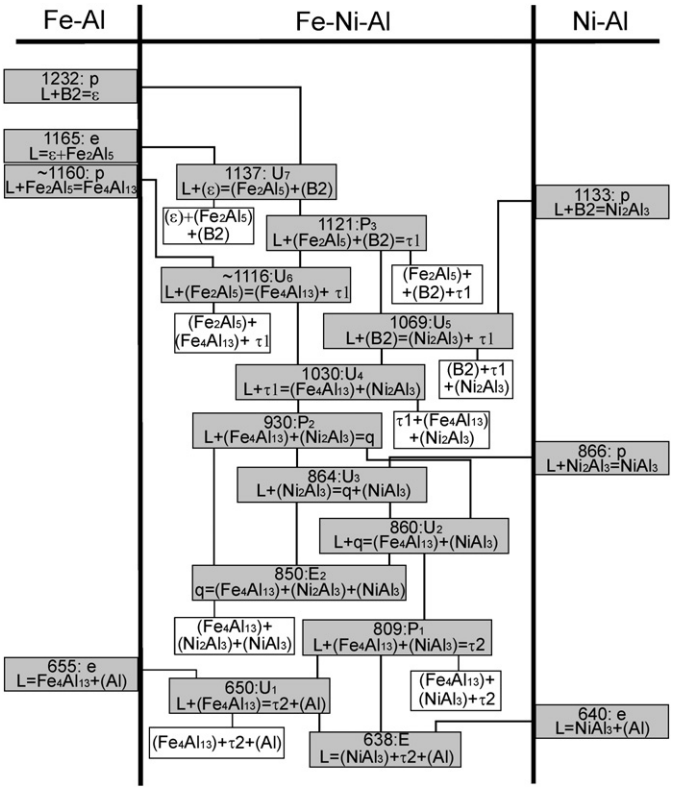

Fig. 6. Partial ternary reaction scheme (Scheil diagram) for Fe–Ni–Al.

3.2. Crystal structure determination of the τ1 ($Fe_{4-x}Ni_xAl_{10}$) and τ2 ($Fe_{2-x}Ni_xAl_9$) ternary compounds

The single crystals used for structure determination were taken from the alloys $Fe_{18.5}Ni_{10}Al_{71.5}$ (τ1) and $Fe_{6.3}Ni_{11.7}Al_{82}$ (τ2). The latter sample was annealed at 750 °C, as τ2 is not stable above 809 °C. The quality of the crystals was examined by the Laue method. Intensity data were then collected at room temperature on a four-circle diffractometer (CAD4) using Mo Kα radiation. The structures were solved by direct methods followed by difference Fourier synthesis and refinements were performed by least-squares methods on F^2. All calculations were carried out with the SHELX–97 package [19]. Final difference Fourier syntheses revealed no significant residual peaks. Crystal data and structure refinement for both compounds are listed in Table 2, atomic coordinates and displacement parameters in Table 3.

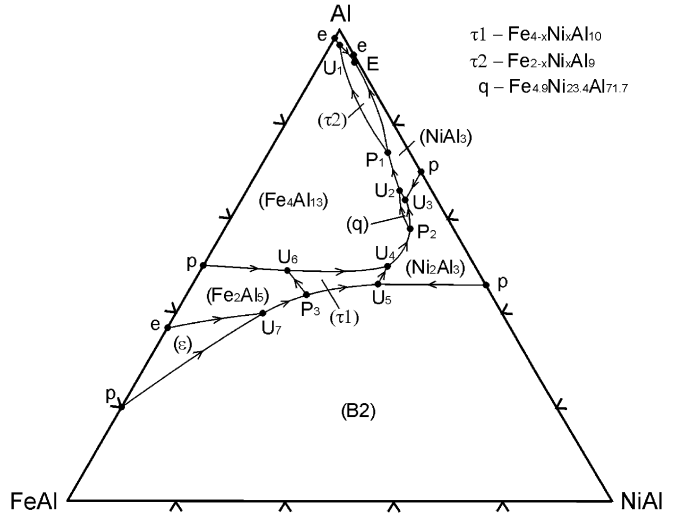

Fig. 7. Liquidus surface projection of Fe–Ni–Al between 50 and 100 at.% Al.

For $Fe_{4-x}Ni_xAl_{10}$ (τ1) the Co_2Al_5-structure type [20] as proposed in Refs. [9,10] was confirmed. Besides the homogeneity range due to Fe/Ni substitution, also a small variability in the Al content could be observed by EPMA: samples situated on the Al-poor side of the τ1 phase generally show around 70.3–70.7 at.% Al, i.e., less than expected for the stoichiometric M_2Al_5-composition (71.4 at.% Al). From our refinement it was found that ~10% of the Al-atoms in the 2*a* site are substituted by Fe/Ni-atoms. The refined composition according to this model corresponds well to the Al-poor composition limit of this compound. A graphical representation of the hexagonal structure and the various coordination polyhedra observed in τ1 are given in Fig. 3. The coordination numbers (CN) of M2 and M3 atoms are 9 and 12, respectively. The coordination polyhedra are trigonal prisms with three additional vertices in front of the side faces (CN = 9) and nearly regular icosahedra (CN = 12). The coordination polyhedra of aluminum are nearly regular icosahedra (M1, CN = 12) and distorted bicapped pentagonal prisms with one (Al2, CN = 13) or two (Al3, CN = 14) additional vertices in front of the side faces.

The ternary phase $Fe_{2-x}Ni_xAl_9$ (τ2) was found to crystallize in the monoclinic structure type Co_2Al_9. This structure type has been found in several binary aluminides and gallides like Co_2Al_9, Rh_2Al_9, Ir_2Al_9, Rh_2Ga_9 and Ir_2Ga_9 [21]. It was found that the gallides crystallize in a slightly distorted version of this structure type (acentric space group *Pc*). The main hint for the distorted version was the strong anisotropy in atomic displacement of the Ga atoms in the space group $P2_1/c$ and the presence of the 050 and 0–50 reflections, which should be systematically absent in this space group [21]. In the case of $Fe_{2-x}Ni_xAl_9$, we don't have any doubts regarding the refinement in the space group $P2_1/c$. Also, the residual values in the space group $P2_1/c$ are lower in comparison with the model refined in the space group *Pc* ($R1[I > 2\sigma(I)] = 0.0335$ and 0.0348, respectively). A representation of the crystal structure of τ2 based on the monocapped square antiprismatic coordination polyhedra [MAl_9] is shown in Fig. 4.

3.3. Ternary phase reactions

The samples annealed at 850 °C and some additional samples annealed at 700 °C and 750 °C were studied by differential thermal analysis (DTA) in order to determine ternary phase reactions within the respective composition range. A graphical representation of phase equilibria within five vertical sections at 80, 75, 71.5, 67 and 60 at.% Al, including experimental data points, is shown in Fig. 5a–e. The experimental data points for thermal effects represent only DTA results obtained on first heating of the annealed samples. The liquidus values were evaluated from the heating- and cooling-curves, respectively.

Altogether, eight previously unknown invariant four-phase equilibria were derived from these data. The peritectic formation of $Fe_{2-x}Ni_xAl_9$ at 809 °C [17,6] and eutectoid decomposition of the decagonal quasi-crystalline phase q [12] was confirmed. The temperature of 865 °C found for the binary peritectic reaction $P1$: $[L + Ni_2Al_3 = NiAl_3]$ is in good agreement with the temperature of 862 °C reported by Gödecke and Ellner [22]. The phase equilibria involving the Fe–Al ε phase in the ternary system need additional investigations. Therefore, the vertical sections at 67 and 60 at.% Al are not complete in the regions below 1137 °C and up to 3.5 and 9 at.% Ni, respectively.

A summary of the invariant reactions derived from DTA data is given in Table 4. This table includes the approximate compositions of the involved phases which are assessed based on a combination of all available experimental data (XRD, EPMA and DTA). A ternary reaction scheme (Scheil diagram) is shown in Fig. 6.

3.4. Liquidus surface

All liquidus values determined by DTA were combined with literature data for the respective binary phase diagrams and the literature data for the ternary close to the Al corner given in [17,23] to yield a liquidus surface projection within the entire investigated composition range. This projection is shown in Fig. 7. The liquidus valleys that separate the different fields of primary crystallization are shown as solid lines with arrows indicating the direction towards lower temperature. The compositions of the liquid phase in the various binary and ternary invariant reactions are shown as black circles in Fig. 7.

Acknowledgements

Financial support from the Austrian Science Foundation (FWF), under the ''Lise-Meitner-Stipendium'', project number M906-B10 and financial support from COST 535 are gratefully acknowledged.

References

[1] Wallin M, Johansson P, Savage S. Mater Sci Eng A 1991;133:307.
[2] George EP, Liu CT, Horton JA, Sparks CJ, Kao M, Kunsmann H, et al. Mater Charact 1997;39:665.
[3] Ono N, Tsukahara A, Kainuma R, Ishida K. Mater Sci Eng A 1999;273–275:420.
[4] Sauthoff G. Intermetallics 2000;8:1101.
[5] Eleno L, Frisk K, Schneider A. Intermetallics 2006;14:1276.
[6] Khaidar M, Allibert CH, Driole J. Z Metallkd 1982;73:433.
[7] Zhang L, Du Y, Xu H, Tang C, Chen H, Zhang W. J Alloys Compd, in press, doi:10.1016/j.jallcom.2006.12.042.
[8] Chumak I, Richter KW, Ipser H. 12th International IUPAC-conference on high temperature materials chemistry HTMC–XII. Vienna, Austria; September 2006.
[9] Bradley AJ, Taylor A. Proc R Soc London Ser A 1938;166:353.
[10] Ellner M, Röhrer T. Z Metallkd 1990;81:847.
[11] Lemmerz U, Grushko B, Freiburg C, Jansen M. Philos Mag Lett 1994;69:141.
[12] Grushko B, Lemmerz U, Fischer K, Freiburg C. Phys Status Solidi A 1996;155:17.
[13] Lemmerz U. Ber Forschungszent Juelich 1996;Juel-3243:124.
[14] Döblinger M, Wittman R, Grushko B. J Alloys Compd 2003;360:162.
[15] Weidner E, Lei JL, Frey F, Wang R, Grushko B. J Alloys Compd 2002;242:156.
[16] de Laissardiere GT, Nguyen-Manh D, Mayou D. Prog Mater Sci 2005;50:679.
[17] Schrader A, Hanemann H. Aluminium 1943;25(10):339.
[18] TOPAS V3, general profile and structure analysis software for powder diffraction data, Bruker AXS, Karlsruhe, Germany; 2005.
[19] Sheldrick GM. SHELXL-97, program for crystal structure refinement and SHELXS-97, program for the solution of crystal structures. Germany: University of Göttingen; 1997.
[20] Burkhardt U, Ellner M, Grin Yu, Baumgartner B. Powder Diffr 1998;13(3):159.
[21] Boström M, Rosner H, Prots Yu, Burkhardt U, Grin Yu. Z Anorg Allg Chem 2005;631:534.
[22] Gödecke T, Ellner M. Z Metallkd 1997;88:382.
[23] Budberg P, Prince A. Aluminium–iron–nickel. updated by Cacciamani G, Ferro R, Grushko B, Perrot P, Schemid-Fetzer R, Light metal ternary systems: phase diagrams, crystallographic and thermodynamic data, Landolt-Börnstein – group IV physical chemistry. In: Light metal systems. Part 2, vol. 11A2. Berlin, Heidelberg: Springer; 2005. pp. 329–358.